# Analysis of chain mechanical characteristics of mine scraper conveyor under material loading and chain clamping conditions

**Chunxue XIE**
Liaoning Technical University
**Zhixiang LIU** ( 380357369@qq.com )
Liaoning Technical University
**Miao XIE**
Liaoning Technical University
**Jun MAO**
Liaoning Technical University

**Article**

**Keywords:** Scraper conveyor, bias load, Chain, finite element analysis

**Posted Date:** March 25th, 2022

**DOI:** https://doi.org/10.21203/rs.3.rs-1457101/v1

# Analysis of chain mechanical characteristics of mine scraper conveyor under material loading and chain clamping conditions

XIE Chunxue[2]*, LIU Zhixiang[1], XIE Miao[1], MAO Jun[1]

(1. Research Institute of mineral resources development and utilization technology and equipment, Liaoning Technical University, Liaoning Province, 123000; 2. School of mechanics and engineering, Liaoning Technical University, Liaoning Province, 123000)

**Abstract:** Taking into account the safety factor of the conventional calculation of chain is in accordance with the two chain to bear external load is calculated, and the actual situation of the two chains of load is not uniform, this paper uses nonlinear dynamic finite element software ABAQUS, the simulation system of scraper chain under bias load, torsional vibration in the process of chain distribution should be produced stress and strain. A torsional vibration model of Kelvin-Voigt scraper chain and system based on the analysis of the vibration characteristics of material loading and clamping the chain scraper chain under torsion. Twist vibration from two adjacent scraper chain as a finite element analysis model of the boundary conditions, the finite element analysis of the stress and strain of the chain, we obtain two kinds of different conditions in the chain link stress strain response and the maximum stress and strain distribution, provide the basis for follow-up in the chain of life prediction, safety factor calculation.

**Key words:** Scraper conveyor; bias load; Chain; finite element analysis

## 0 Introduction

The working process of the scraper conveyor is affected by many factors, such as environment, working condition, fault and so on. its external excitation mainly includes three aspects: The resistance between scraper and material, that is, the excitation of cargo load. The friction and collision force between scraper and the middle slot along the conveyor, that is, line shape excitation. The impact force caused by card chain accident, that is, card chain fault excitation.

In his research on the driving device of scraper conveyor, Sikora W [1] puts forward that when it is subjected to non-uniform load, the power balance of the system determines the working characteristics of the driving device. Murphy C J [2]makes an in-depth study on the dynamic load characteristics of scraper conveyor, on the basis of which a new method is designed to describe the load change of scraper conveyor in real time. Katterfeld A. and Gr ö ger T [3]mainly studied the material loading process and material unloading process of the scraper conveyor, and the discrete element method was used to simulate the two working processes. The simulation results are in good agreement with the experimental results. Dolipsk M [4] established the dynamic model of scraper conveyor under non-uniform load and obtained the slip rate of motor in this state.

Li Weikang [5] based on the mechanism of chain running resistance under extreme working conditions, the derivation formula of chain running resistance is obtained, and the distance between scrapers is optimized by minimizing the running resistance. Xu Guangming and Yang Weihong [6] put forward a new method to calculate the resistance pretension of scraper chain under different driving conditions, and analyzed the influence of different scraper conveyor structure on resistance calculation coefficient. Han Dejiong [7] studied the change of running resistance coefficient of upper section (bearing section) and lower section (return section) with the change of traction chain speed. Liu Wensheng [8] put forward a concrete scheme to solve the practical factors affecting the running resistance of the scraper conveyor.

Ma Shuhuan [9] studied the influence of the change of the load of the scraper conveyor on the dynamic characteristics of the scraper conveyor. With the combination of theory and practice, the

distribution law of the scraper conveyor under different operating conditions, running time and load was analyzed, and the distribution law was applied to the solution of the dynamic equation. Cai Liu [10] combines the finite element method with the discrete element method, gives full play to the advantages of the two algorithms, studies the dynamic characteristics of the material in the middle trough of the scraper conveyor, and studies the force function and transportation state of the material in detail. the force and motion state of material and material, material and boundary are obtained. Liu Wei[11] divided the scraper chain into heavy section and light section, and analyzed the running resistance of the two sections. Wang Yabin [12] made an in-depth study on the total operation resistance of the scraper conveyor, and established the model of power balance control system driven by double motor and carried out simulation analysis.

Under the action of bias load, the scraper chain system will produce torsional pendulum, resulting in uneven force on the two chains. The conventional chain safety factor (load factor) is calculated according to the external load of two chains. Therefore, when the scraper chain system produces torsion pendulum, it is possible to cause one chain force and another chain not, so that the force chain may exceed the safety load, resulting in chain breakage accidents that often occur in the scraper conveyor.

Therefore, this paper studies the operation resistance of scraper conveyor considering the characteristics of material distribution. The nonlinear dynamic finite element software ABAQUS is used to simulate the distribution of stress and strain in the process of torsional pendulum vibration of scraper chain system under bias load, which provides a basis for chain life prediction and safety factor calculation.

## 1 Working condition analysis of scraper conveyor

The main working principle of the scraper conveyor is to take the chute as the bearing member of the coal. The scraper fixed on the chain as its traction component, and the driving device to drive the sprocket to rotate so as to make the scraper chain run. In the process of operation, the scraper conveyor will overcome the friction between the chute and the bottom plate, promote the material to move along the chute, and complete the transportation of materials[10-12].

The scraper conveyor is usually in the form of double drive at the head and tail, as shown in figure 1. The head of the machine is the driving part, which is mainly composed of the head frame, the sprocket assembly, the drive system and the middle part. The head of the machine not only has the function of providing power for the transportation system, but also has the functions of tight chain and supporting accessories. The drive system of scraper conveyor consists of three asynchronous motors, hydraulic couplers and reducers. The coupling device of the conveyor is a hydraulic coupler, which can effectively adjust the output characteristics of the motor and protect the motor when used with the asynchronous motor, and the reducer can realize the function of reducing speed and increasing torsion. high-power planetary reducers are usually used [13-14].

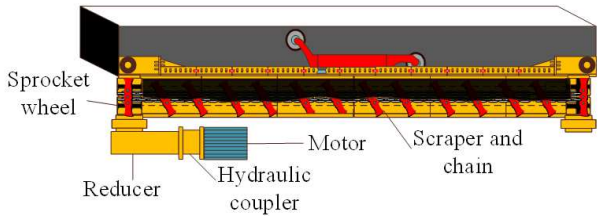


Figure 1 Chain transmission system of Mine Scraper Conveyor

Material loading load and chain load are the most common external excitation loads of scraper conveyor chain.

### 1.1 Analysis of material loading conditions

#### 1.1.1 Analysis of material running resistance

At present, the double helix drum shearer is mostly used for two-way reciprocating mining in coal mining, and the turning of the double helix drum is generally opposite, that is, forward rotation and reverse rotation. The forward opposite rotation refers to the rotation of the front and rear spiral drum of the shearer toward the center of the shearer. Reverse rotation refers to the outward rotation of

the front and rear spiral drum of the shearer. It is generally believed that the material distribution of coal and rock cut by shearer drum in fully mechanized mining face is shown in figure 2.

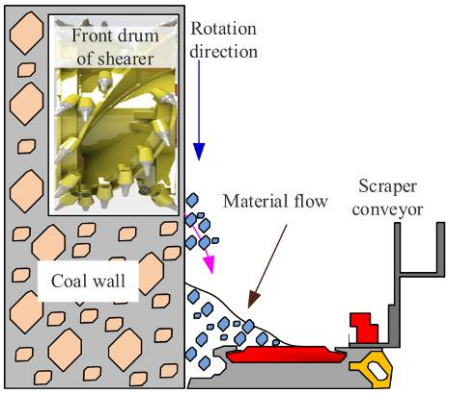


Figure 2 Distribution of coal and rock in drum cutting

Through the analysis and study of the coal loading mechanism of the shearer and the accumulation mechanism of coal bulk materials, the distribution characteristic curve of coal bulk materials on the cross section of the scraper conveyor in the working face can be obtained. After the coal block material is cut by the shearer spiral drum and loaded on the scraper conveyor, the coal block material almost does not have the sub-speed along the direction of the conveyor. Under the action of scraper and chain, coal block material gradually accelerates to the same running speed as scraper and chain. In this process, the scraper and the chain bear the friction force from the middle trough bottom plate, the coal wall side static material and the coal baffle that need to be overcome when the coal block material runs from static to the same speed. Because the initial time distribution of coal lump material in the cross-section direction of the scraper conveyor is uneven, this results in the bias load on the scraper and chain.

The running resistance of the coal lump material mainly comes from the friction resistance $f_1$ between the coal lump material and the middle trough bottom plate, the friction resistance $f_2$ between the coal lump material and the coal retaining plate, and the friction resistance $f_3$ between the moving coal lump material and the static material on the side of the coal wall. The running resistance analysis diagram of stable coal lump material before collapse is shown in figure 3.

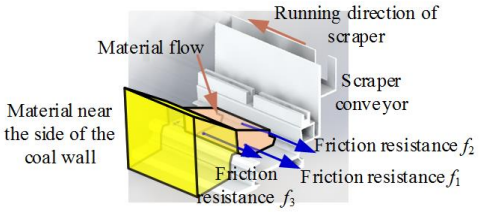


Figure3 Analysis of coal material running resistance

The friction resistance $f_1$ between the bottom plate of the middle tank and the coal lump material is expressed as follows:

$$f_1 = \mu_c \int_0^L y(x) g l_s \rho \mathrm{d}x \tag{1}$$

Where $\mu_c$ is the friction coefficient between the bottom plate of the middle trough and the coal lump material, and $l_s$ is the length of the material along the direction of the conveyor, m.

The friction resistance $f_2$ between the coal baffle and the coal block material is expressed as the product of the lateral pressure of the coal lump material to the coal baffle and the friction resistance coefficient:

$$\begin{aligned} f_2 &= \mu_c n_s N_{x1} = \mu_c n_s \rho g L l_s h_1 \\ &= \mu_c n_s \rho g L l_s y(L) \end{aligned} \tag{2}$$

Where $n_s$ is the lateral pressure coefficient of the coal lump material to the coal baffle, $n_s=(1+\sin\varphi_s)/(1-\sin\varphi_s)=\tan^2(45^\circ+\varphi_s/2)$; $\varphi_s$ is the internal friction angle of the bulk material, °; $N_{x1}$ is the positive pressure of the coal lump material on the side of the coal baffle; $h_1$ is the height of the coal lump material on the side of the coal baffle, m, if $h_1=0$, then there is no friction resistance between the coal baffle and the coal block material.

The friction resistance $f_3$ between the moving coal lump material and the static coal lump material on the side of the coal wall is expressed as the product of the lateral pressure and the friction resistance coefficient of the moving coal lump material to the static coal lump material.

$$\begin{aligned} f_3 &= \mu_c n_s N_{x2} = \mu_c n_s \rho g L l_s h_2 \\ &= \mu_c n_s \rho g L l_s y(0) \end{aligned} \tag{3}$$

Where $N_{x2}$ is the positive pressure of the coal lump material on the side of the coal wall, $h_2$ is the

height of the coal lump material on the coal wall side, and m, if $h_2$=0, then the friction resistance $f_3$ between the moving material and the still material on the coal wall side is zero.

### 1.1.2 Analysis of running resistance of scraper

During the operation of the scraper conveyor, the chain and scraper will rub against the bottom plate of the middle slot, resulting in friction resistance. It is one of the main running resistance of long-distance scraper conveyor, which needs to be overcome by driving motor. Therefore, it can not be ignored. The friction resistance of the scraper in the middle groove is shown in figure 4.

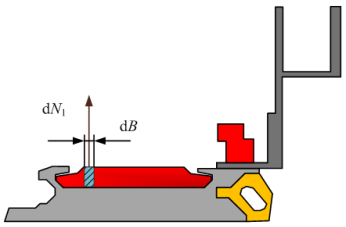


(a) There is no coal block material cover above the scraper.

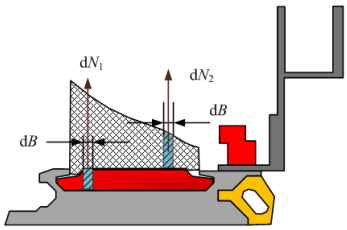


(b) The scraper is completely covered with coal lump material

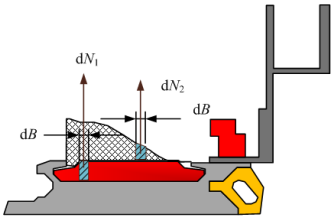


(c) The scraper is partially covered with coal lump material.

Figure 4 Sketch of friction resistance of scraper running

Along the transverse direction of the scraper, the pressure of the gravity of the scraper itself on the middle trough bottom plate is:

$$\mathrm{d}N_1 = \gamma_1 \mathrm{g} \cdot \mathrm{d}B \tag{4}$$

Where $\gamma_1$ is the weight of the length of the scraper unit, kg/m.

The pressure of the coal block material above the scraper on the scraper only considers the volume of the material directly above the scraper, then the positive pressure of the material per unit length of the scraper is:

$$\mathrm{d}N_2 = \rho \mathrm{g} \mathrm{d}V = \rho \mathrm{g} b h \cdot \mathrm{d}B \tag{5}$$

Where $b$ is the length of the scraper. $h$ is the height of the bulk material of the coal block directly above the scraper, m. It is actually a dynamic function related to the working mode and running time of the shearer. According to the relevant parameters such as coal loading mechanism and running time of the shearer, the characteristic curve of material distribution in the middle trough section of the required position is obtained, and the value of h is determined.

To sum up, the total friction resistance of the scraper of the unit section is:

$$\mathrm{d}F_j = \mu \mathrm{d}N_1 + \mu \mathrm{d}N_2 = \mu\left(\gamma_1 \mathrm{g} + \rho \mathrm{g} b h\right)\mathrm{d}B \tag{6}$$

### 1.1.3 Analysis of chain running resistance

The drag chain friction resistance of the chain in the middle groove is shown in figure 5.

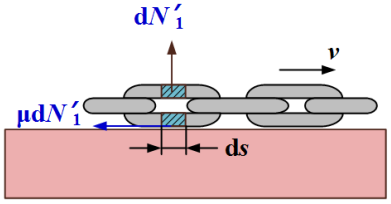


(a) No coal lump material cover above the chain

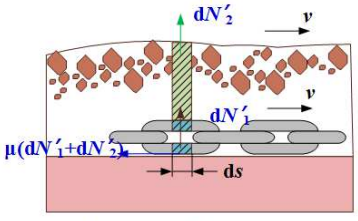


Longitudinal section view

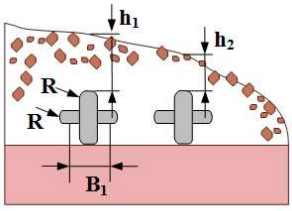


Middle slot section view

(b) the chain is covered with coal lump material

Figure5 Sketch of friction resistance of chain running

The pressure of the gravity of the chain itself per unit length on the middle trough floor is as

follows:

$$dN_1' = \gamma_2 g \cdot ds \tag{7}$$

Where $\gamma_2$ is the weight per unit length of the chain, kg/m; $s$ is the distance between the two scrapers, m.

The pressure of the coal lump material on the chain only considers the volume of the material directly above the chain. So the positive pressure exerted by the material on the chain per unit length is:

$$\begin{aligned} dN_2' &= \rho g dV' \\ &= \rho g\left(\frac{B_1 + 2R + 2R}{2}\right) h_i ds, \quad i=1,2 \end{aligned} \tag{8}$$

Where $B_1$ is the distance between two straight bars of a single chain, m; $R$ is the radius of the ring chain, m; $h_i$ is the height of the bulk material of coal lump directly above the chain, m, where the lower corner $i$=1 or $i$=2 represent the first chain or the second chain, respectively. $h_i$ is actually a dynamic function related to the working mode and running time of the shearer. According to the coal loading mechanism, running time and other relevant parameters of the shearer, the material distribution characteristic curve of the middle trough section of the required position is obtained, and the value of $h_i$ is determined.

To sum up, the total friction resistance of the chain of the unit segment is:

$$\begin{aligned} dF_i &= \mu dN_1' + \mu dN_2' = \\ &\mu\left(\gamma_2 g + \rho g\left(\frac{B_1 + 2R + 2R}{2}\right) h_i\right) ds \\ &, \quad i=1,2 \end{aligned} \tag{9}$$

## 1.2 Analysis of the working condition of the clip chain

Both unilateral and bilateral chains will have a great impact on the chain. Among them, one side of the chain will produce scraper partial load, which makes the chain on the side of the chain suffer a greater impact. The working condition of the card chain can be simulated by limiting the running speed of the side scraper of the card chain or increasing the impact load on the side of the card chain, as shown in figure 6.

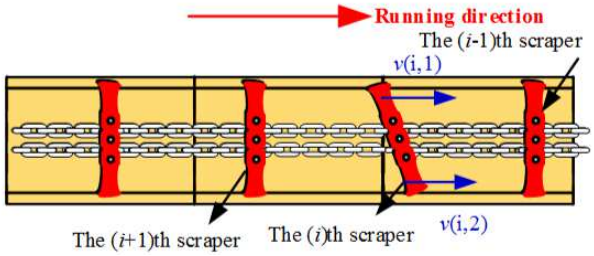


(a) Limit the running speed of side scraper of card chain

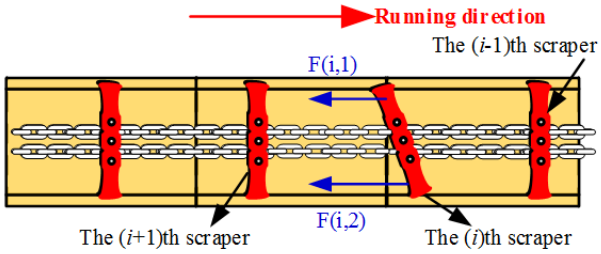


(b) Increase the impact load on the side of the chain

Figure6 Simulation of chain blocked

The method of increasing the impact load on the side of the chain to simulate the abnormal load of the chain can be simulated in the following ways [13]:

$$F(i,j)(t) = \begin{cases} 0 & t = 0^- \\ F(i,j)_{(0)}\left(\frac{t}{T}\right) & 0 \le t \le T \\ F(i,j)_{(0)} & t \ge T \end{cases} \text{ Linear type (10)}$$

$$F(i,j)(t) = \begin{cases} 0 & t = 0^- \\ F(i,j)_{(0)}\left(e^{-(t-T)}\right) & 0 \le t \le T \\ F(i,j)_{(0)} & t \ge T \end{cases} \text{ Exponential type (11)}$$

$$F(i,j)(t) = \begin{cases} 0 & t = 0^- \\ F(i,j)_{(0)} & t = 0^+ \end{cases} \text{ Mutant type (12)}$$

In the formula, $i$ means the $i$th scraper is stuck; $j$ means the stuck side.

The working condition of the chain can be described by defining the movement of the scraper at a certain point, which can be described in the following ways: if one end of the $I$ scraper is stuck, the initial speed of the side scraper is $v_i(0)$, and the speed $v_i(t)$ of the scraper after being stuck can be described in the following forms:

$$v_i(t)=\begin{cases} v_{i(0)} & t=0^- \\ v_{i(0)}(1-\dfrac{t}{T}) & 0\le t\le T \\ 0 & t\ge T \end{cases}$$ Linear type (13)

$$v_i(t)=\begin{cases} v_{i(0)} & t=0^- \\ v_{i(0)}(1-e^{-(t-T)}) & 0\le t\le T \\ 0 & t\ge T \end{cases}$$ Exponential type(14)

$$v_i(t)=\begin{cases} v_{i(0)} & t=0^- \\ 0 & t=0^+ \end{cases}$$ Mutant type (15)

## 2 Torsional pendulum vibration model of scraper chain system

By using the finite element method, the double chain drive system of scraper conveyor is divided into several units, and each of which is connected by Kelvin-Voigt model. Then the longitudinal discretization dynamic model of chain drive system considering torsional pendulum excitation is established [13], as shown in figure 7.

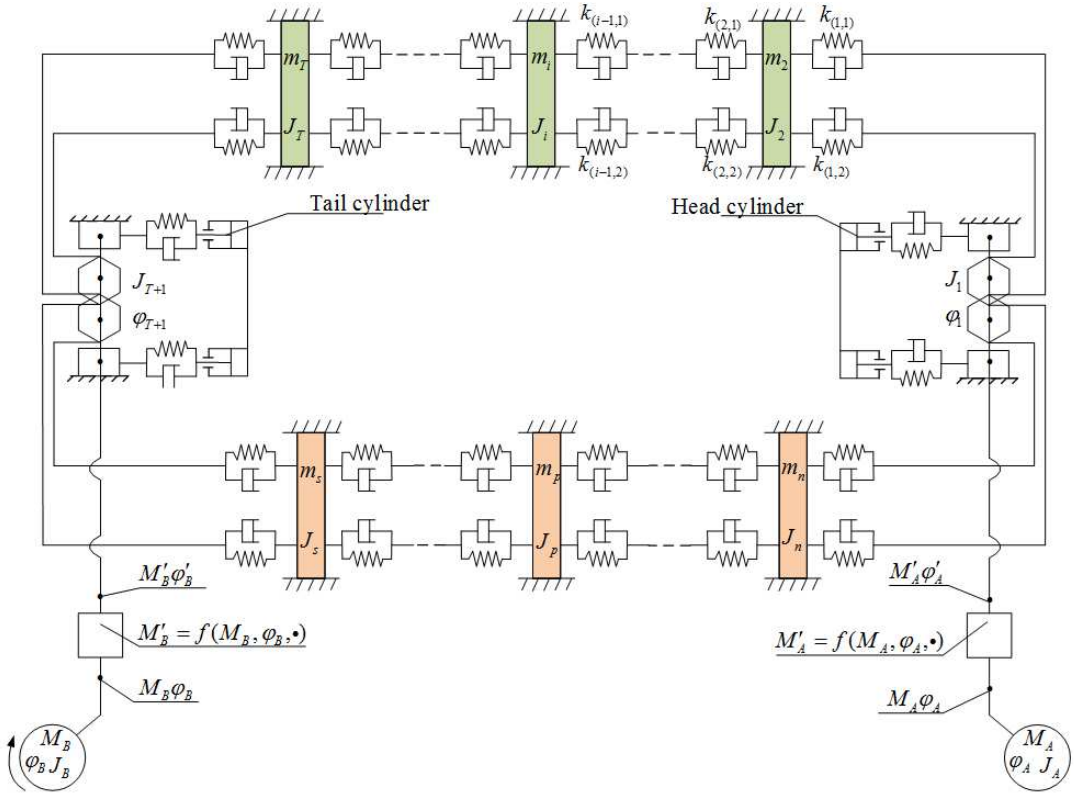


Figure 7 Longitudinal dispersion dynamic model of the chain transmission system with considering the effect of incentive

The dynamic differential equation is established according to the longitudinal discretization dynamic model of the chain drive system considering the torsional pendulum excitation shown in figure 7.

$$
\begin{cases}
J_A\ddot{\varphi}_A + k_A(\varphi_A - \varphi_1) + c_A(\dot{\varphi}_A - \dot{\varphi}_1) = M_A \\
J_1\ddot{\varphi}_1 + k_A(\varphi_1 - \varphi_A) + c_A(\dot{\varphi}_1 - \dot{\varphi}_A) + (F_{1(t)} - F_{n(t)})R_A = 0 \\
\dfrac{d(m_2\dot{x}_2)}{dt} - F_1(t) + F_2(t) + W_2 = 0 \\
\mathbf{M} \\
J_B\ddot{\varphi}_B + k_B(\varphi_B - \varphi_{i+2}) + c_B(\dot{\varphi}_B - \dot{\varphi}_{i+2}) = M_B \\
J_n\ddot{\varphi}_n + k_B(\varphi_{i+2} - \varphi_B) + c_B(\dot{\varphi}_{i+2} - \dot{\varphi}_B) + (F_{i+2} - F_{i+1})R_n = 0 \\
\dfrac{d(m_{i+3}\dot{x}_{i+3})}{dt} + F_{i+3(t)} - F_{i+2(t)} - W_{i+3} = 0 \\
\mathbf{M} \\
\dfrac{d(m_n\dot{x}_n)}{dt} + F_{n(t)} - F_{n-1(t)} - W_n = 0 \\
F_{1(t)} = k_1(\varphi_1 R_1 - x_2 - x_{n+1}) + c_1(\dot{\varphi}_1 R_1 - \dot{x}_2 - \dot{x}_{n+1}) \\
F_{j(t)} = k_j(x_j - x_{j+1}) + c_1(\dot{x}_j - \dot{x}_{j+1}) \qquad i \geq j \geq 2 \text{或} n-1 \geq j \geq i+3 \\
F_{i+1(t)} = k_{i+1}(x_{i+1} - \varphi_{i+2}R_{i+2} + x_{k+2}) + c_{i+1}(\dot{x}_{i+1} - \dot{\varphi}_{i+2}R_{i+2} + \dot{x}_{k+2}) \\
F_{i+2(t)} = k_{i+2}(\varphi_{i+2}R_{i+2} + x_{k+2} - x_{i+3}) + c_{i+2}(\dot{\varphi}_{i+2}R_{i+2} + \dot{x}_{k+2} - \dot{x}_{i+3}) \\
F_{n(t)} = k_n(x_n - \varphi_1 R_1 + x_{n+1}) + c_n(\dot{x}_n - \dot{\varphi}_1 R_1 + \dot{x}_{n+1})
\end{cases}
\tag{16}
$$

Among them, taking the dynamic tension of each unit section connection point chain as the connection variable, the transient dynamic tension is obtained by solving the longitudinal expansion dynamic model. Taking the transient dynamic tension as the total tension of the two chains in the unit section where the torsional pendulum vibration excitation is applied, the torsional pendulum vibration characteristics of the scraper chain system in the unit section are solved. If the torsional pendulum vibration excitation is applied in the *i*th scraper unit section, the torsional pendulum dynamic model of the scraper chain system inside the *i*th unit section is established as the torsional pendulum dynamic model, as shown in figure 8.

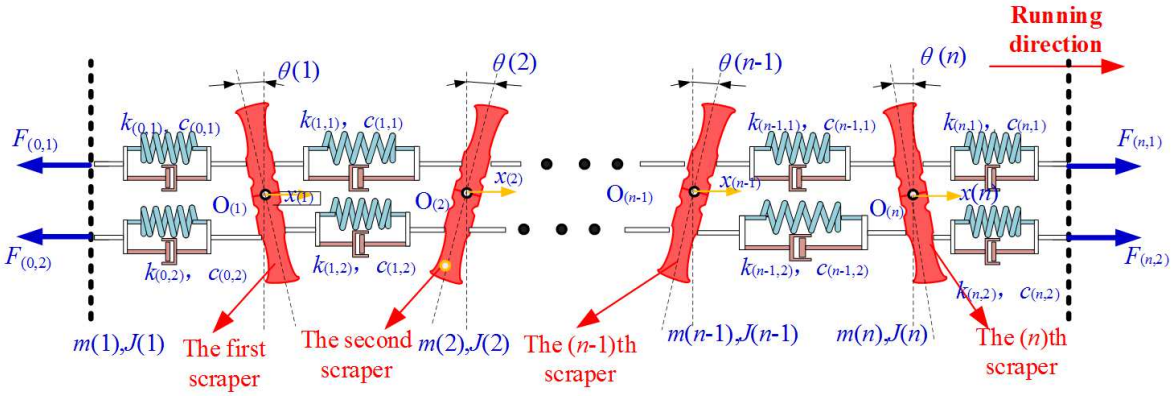


Figure8 Analysis model of torsional vibration system of scraper chain

The differential equation of motion is established for the *i*th scraper in the torsional pendulum vibration analysis model of scraper chain system [14]:

$$
\begin{cases}
m_i\ddot{x}_i = F_{d(i,1)} + F_{d(i,2)} + F_{J(i,1)} + F_{J(i,2)} \\
\qquad - F_{d(i\text{-}1,1)} - F_{d(i\text{-}1,2)} - F_{J(i\text{-}1,1)} - F_{J(i\text{-}1,2)} - W_{(i)} \\
J_i\ddot{\theta}_i = \left(F_{J(i,1)} + F_{d(i,1)} + F_{J(i\text{-}1,2)} + F_{d(i\text{-}1,2)}\right)h_1 \\
\qquad -\left(F_{d(i,2)} + F_{J(i,2)} + F_{d(i\text{-}1,1)} + F_{J(i\text{-}1,1)}\right)h_2 - W_{(i)} \cdot h
\end{cases}
\tag{17}
$$

Taking MG500/1130- WD shearer and SGZ1000/ 1050 scraper conveyor as examples, the applied load is simplified into three parts: The first part is the friction force between the material and the bottom plate, which is equivalent to a concentrated load acting on the middle of the scraper; the second part is the friction force between the material and the coal baffle, which acts on one side of the scraper; the third part is the friction force

between the material and the coal wall, acting on the other side of the scraper. All three part loads are set to a step load and applied to the 15th scraper of the analytical model. The dynamic response characteristics of the scraper chain system are solved numerically by matlab, and the simulation results are shown in figure 9.

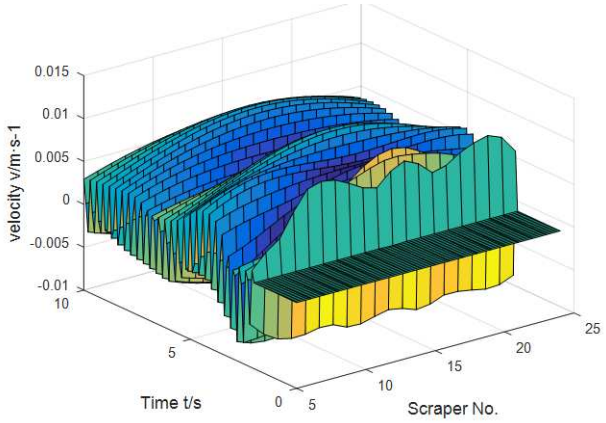


(a) Simulation results of vibration velocity of scraper

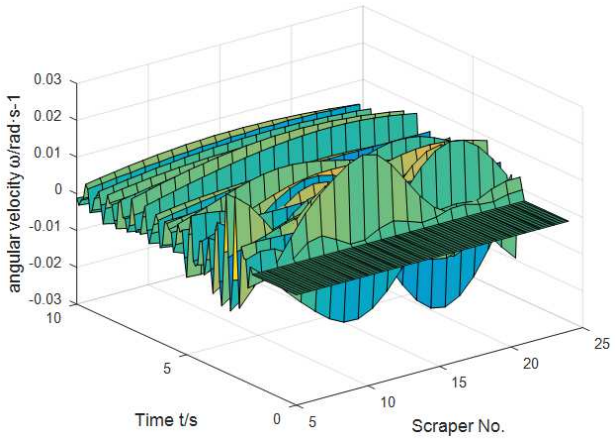


(b) Simulation results of angular velocity of scraper torsional pendulum

Figure 9 Dynamic response analysis model of the scraper chain system in the process of material loading without material running ahead

The sudden clip chain load is applied on the edge of the scraper, and the dynamic response characteristics of the whole scraper chain system are solved numerically by matlab, and the simulation results are shown in figure 10.

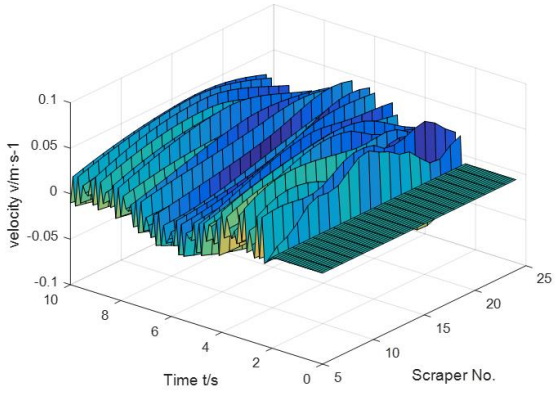


(a) Simulation results of vibration velocity of scraper

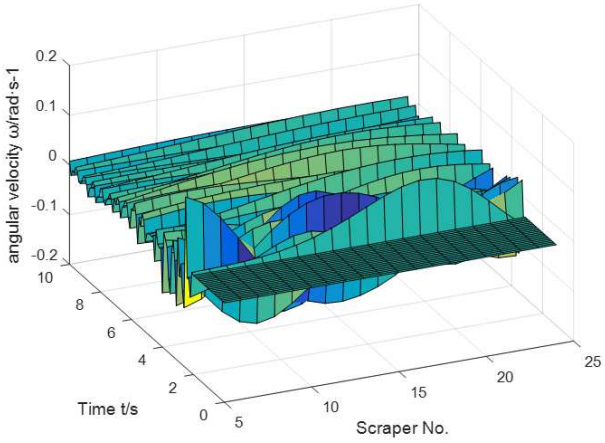


(b) Simulation results of angular velocity of scraper torsional pendulum

Figure 10 Dynamic response analysis model of the scraper chain system in the process of material loading without material running ahead

# 3 Boundary conditions for numerical simulation of ring chain drive

In the previous paper, the torsional pendulum vibration characteristics of scraper and chain system of conveyor under different working conditions are analyzed theoretically and simulated, and the changes of speed and angle of scraper torsional pendulum vibration under material loading and chain conditions are obtained. Here, the most representative material loading conditions and the chain clamping conditions which have great influence on the chain tension are selected as the working conditions for the numerical simulation of the ring chain transmission process in this chapter.

The calculation results of the torsional pendulum vibration of one of the chains and scrapers obtained under the selected working conditions are extracted and used as the load for the numerical simulation of the ring chain transmission process. Under this load and boundary condition, the change of stress field in the process of ring chain transmission is studied, and the influence of torsional pendulum vibration load on the stress and strain of ring chain is analyzed. It provides a basis for chain life prediction and safety factor calculation.

## 3.1 Load applied under material loading condition

During the operation of the scraper conveyor in the fully mechanized mining face, the material loading condition occurs all the time. The load of the ring chain in the transmission process mainly comes from the material loading process, while the loads such as chain clamping and chain breaking belong to extreme working conditions. In the material loading process obtained above, the vibration displacement and torsion angle of the scraper at both ends of the 20th section of the chain are selected as the boundary conditions to add static tension and friction related to the running state of the chain. The time-varying curves of the vibration displacement and torsion angle of the scraper at both ends are shown in figure 11.

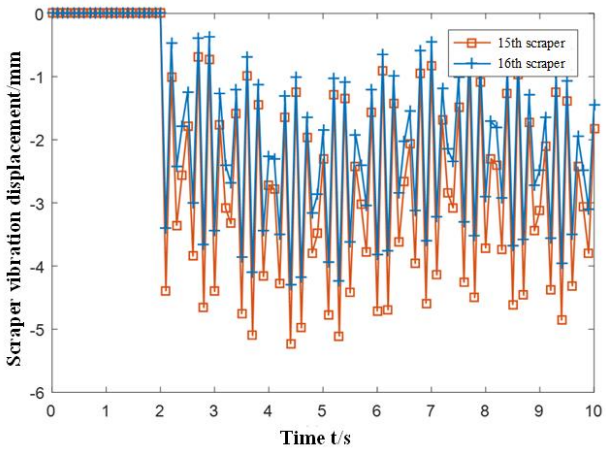


(a) Variation curve of scraper vibration displacement with time

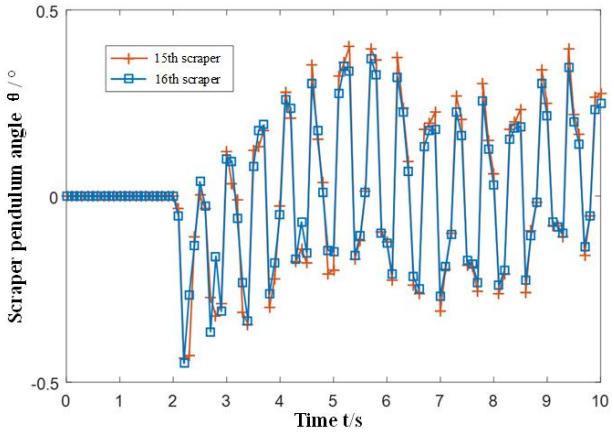


(b) Variation curve of scraper torsional pendulum vibration angle with time

Figure 11 Curve of vibration displacement and angle of material loading

## 3.2 load is applied under the condition of card chain

During the operation of the scraper conveyor in fully mechanized mining face, the scraper is often stuck by a large piece of material. The working condition of the chain is a common extreme condition, which has a great loss for the chain. The working condition of the chain obtained above is selected, and the vibration displacement and torsion angle of the scraper at both ends of the 20th section of the chain are selected as the boundary conditions to add static tension and friction force related to the running state. The time-varying curves of vibration displacement and torsion angle of the scraper at both ends are shown in figure 12.

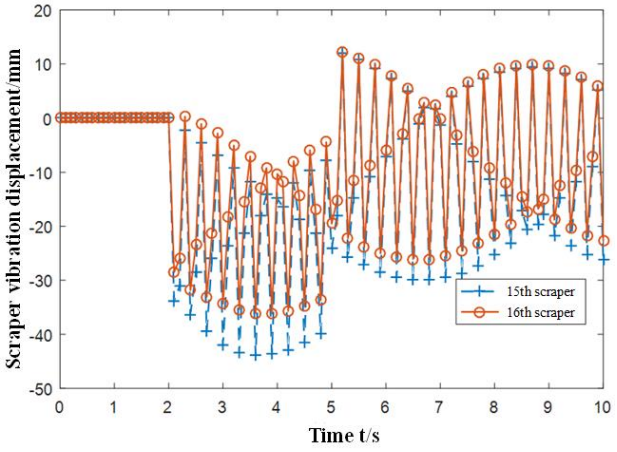


(a) Variation curve of scraper vibration displacement with time

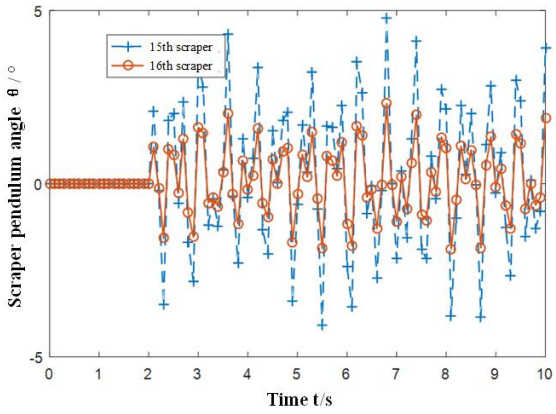


(b) Variation curve of scraper torsional pendulum vibration angle with time

Figure 12 Curve of vibration displacement and angle of material loading

# 4 Finite element analysis of chain contact

## 4.1 Establishment of finite element model of chain contact

In this paper, taking the Φ 38 × 137 chain link of SGZ1000/ 1050 scraper conveyor as the research object, two ring chains are established, and the ring chain is composed of 9 chains in contact with each other. The dynamic simulation of the instantaneous contact process of the circular chain under the boundary condition of torsional pendulum vibration is carried out. The nonlinear dynamic finite element software ABAQUS is used to establish the finite element model for numerical simulation of circular chain transmission process under the action of scraper chain torsional pendulum vibration, as shown in figure 13.

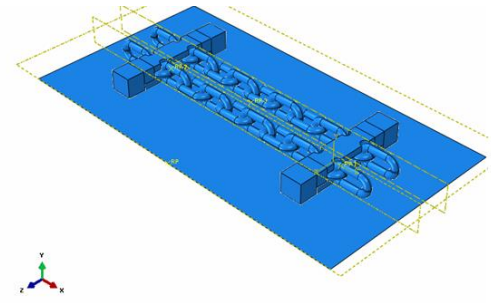

Figure13 Numerical simulation finite element model of transmission process of circular endless chain under torsional vibration of scraper chain

23MnNiCrMo is widely used in mining circle chain. Its Poisson's ratio, Young's elastic modulus, density and shear modulus are 0.25, $2.06\times10^{11}$Pa, $77.86\times10^{-6}$kg • $mm^{-3}$ and $5.6\times10^{5}$Pa respectively. The finite element model is meshed, boundary conditions are applied and loads are applied. The finite element model of the ring chain mold is meshed using the C3D8R element type with high precision in the ABAQUS software, and the refined mesh is used to deal with the contact position between the ring chains [15]. A total of 155476 grids are divided in the analytical model.

## 4 .2 Analysis of numerical simulation results

### 4.2.1 Analysis of numerical simulation results of material loading condition

The finite element analysis and calculation of the ring chain transmission process under the material loading condition is carried out, and the stress and strain changes of each chain link between the two scrapers are obtained. The Mises stress distribution of the chain between the two scrapers at different times of 1s, 3s, 5s, 7s and 9s is shown in figure 14 and the maximum strain distribution is shown in figure 15.

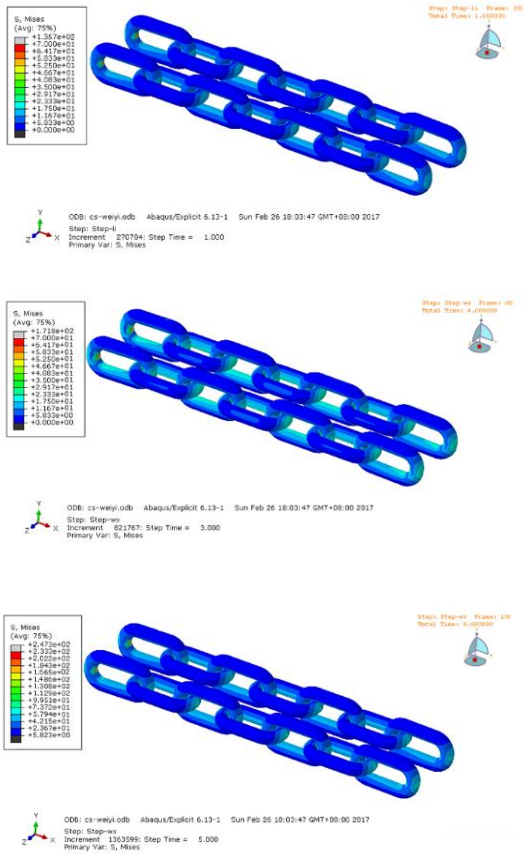

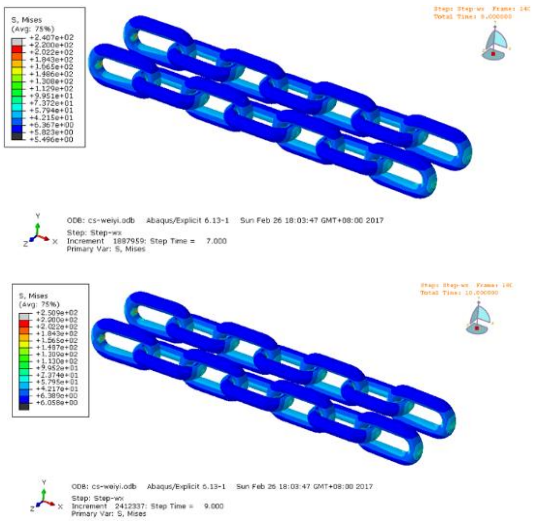

Figure14 The Mises stress distribution of the chain between the two scrapers

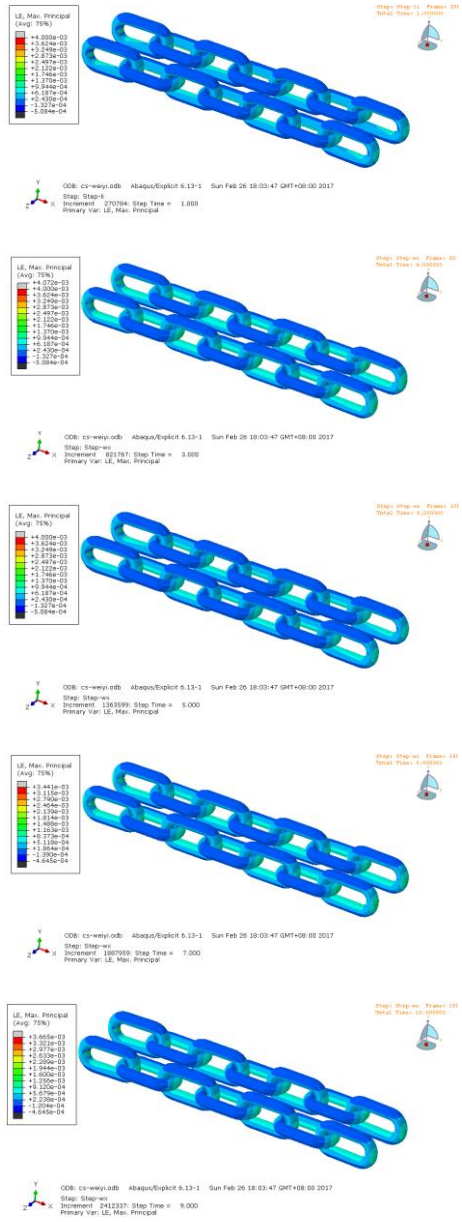

Figure15 The maximum strain distribution of the chain between two scrapers

With the change of time, the chain has a slight twist under the influence of scraper torsional pendulum vibration, but the effect is relatively small. The inner side of the chain produces strain under the action of compressive stress, and the outside of the chain produces strain under the action of tensile stress. The stress and strain at the contact part between the link and the link is the largest, and the maximum stress is 2.50e+2MPa, which becomes 4.07e-3. In the process of material loading, the running resistance of the chain near the front is increased, and the rear chain is forced to pull, collide with each other and transmit vibration, resulting in stress concentration at the contact of the chain link. The stress and the resulting strain in the arc segment of the chain are more obvious. Different monitoring points are selected on the two chains in order to more directly observe the changes of stress and strain with time. Select the position of the monitoring point in the chain as shown in figure 16.

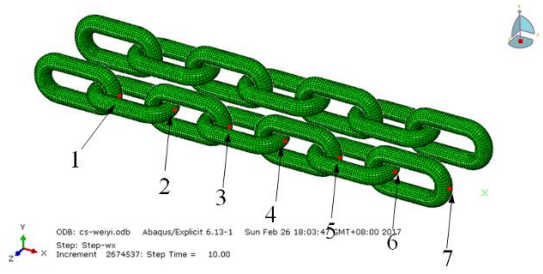


(a) Position of monitoring point in chain 1

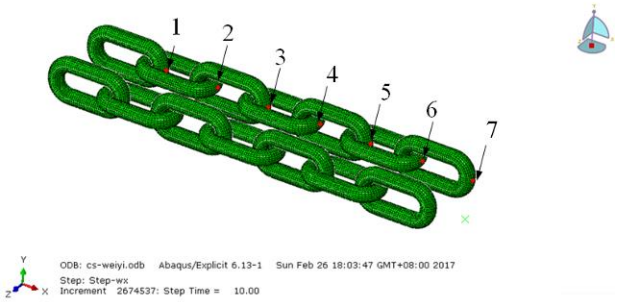


(b) Position of monitoring point in chain 2

Figure 16 Select the location of monitoring points in the chain

The stress and strain changes over time at the monitoring points in chains 1 and 2 are shown in figures 17 and 18.

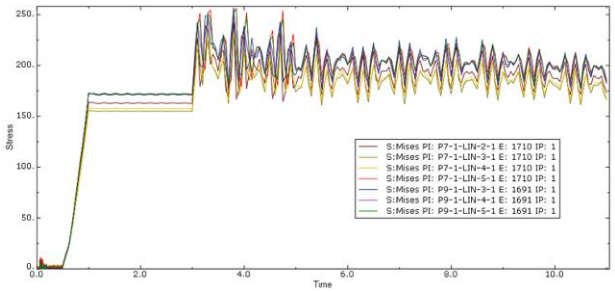


(a) Stress change

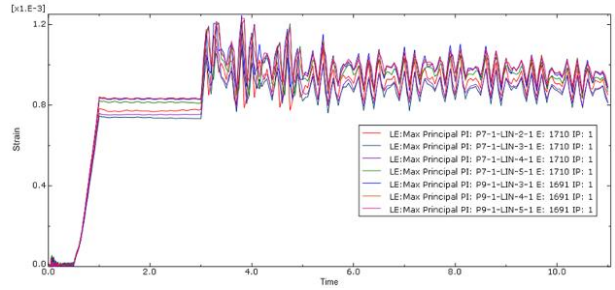


(b) Strain change

Figure 17 The change of stress and strain in each of the monitoring points in chain 1 under the working condition 1

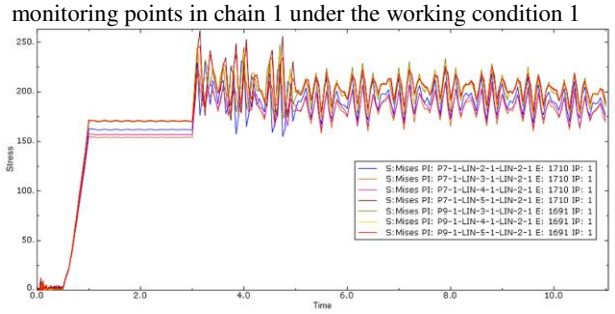


(a) Stress change

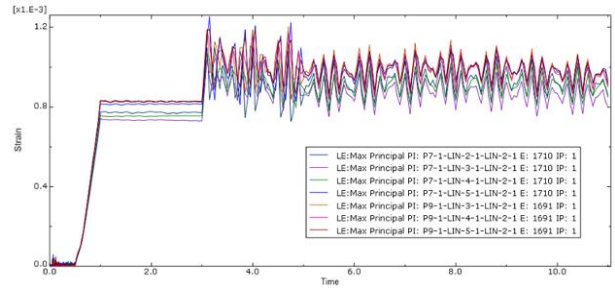


(b) Strain change

Figure 18 The change of stress and strain in each of the monitoring points in chain 2 under the working condition 1

Through the analysis of the time variation curves of the stress and strain of each monitoring point in chain 1 and chain 2, it is known that the stress and strain of the chain monitoring point remain constant during 1.0-3.0s, because the working condition set at this time is that there is no material loading. At this time, the stress and strain of each chain monitoring point are also different, so there is friction between the chain and the bottom plate through the software, which is more in line with the real working conditions. Therefore, the stress and strain of each monitoring point increases gradually, and the more forward the chain monitoring point, the greater the stress and strain. Similarly, during the period of 3.0 to 10.0s, the stress and strain of each monitoring point of the chain during the material loading process is also the same, the closer to the position of the front scraper, the greater the amplitude of stress and strain fluctuation. The maximum stress is concentrated in the first three fluctuation peaks. Under the material loading condition, the maximum stress in the first chain monitoring point is 258.5MPa, the second chain monitoring point is 270.6MPa, the maximum strain value in the first chain monitoring point is 1.25e-3, and the maximum strain value in the second chain monitoring point is 1.32e-3. Under the condition of material loading, it can cause slight torsional pendulum vibration of the scraper chain system, and make the stress and strain of each link in the chain fluctuate. Although the stress and strain of the two links in the corresponding position of the two chains are not much different, the loading material load is the type of load excitation with the highest frequency in the use of the chain. Long-term unbalanced material partial load will cause the stress and strain difference of the two links in the corresponding position of the two chains to become larger and larger, and finally cause one of the chains to break, followed by the two chains to break. Therefore, the research content of this section can provide a certain basis for the study of chain life prediction under long-term material bias load.

### 4.2.2 Analysis of numerical simulation results of clip chain condition

The finite element analysis and calculation of the transmission process of the ring chain under the condition of the clip chain is carried out, and the stress and strain change of the chain link between the two scrapers is obtained. The Mises stress distribution of the chain between the two scrapers at different times of 1s, 3s, 5s, 7s and 8s after loading is shown in figure 19 and the maximum strain distribution is shown in figure 20.

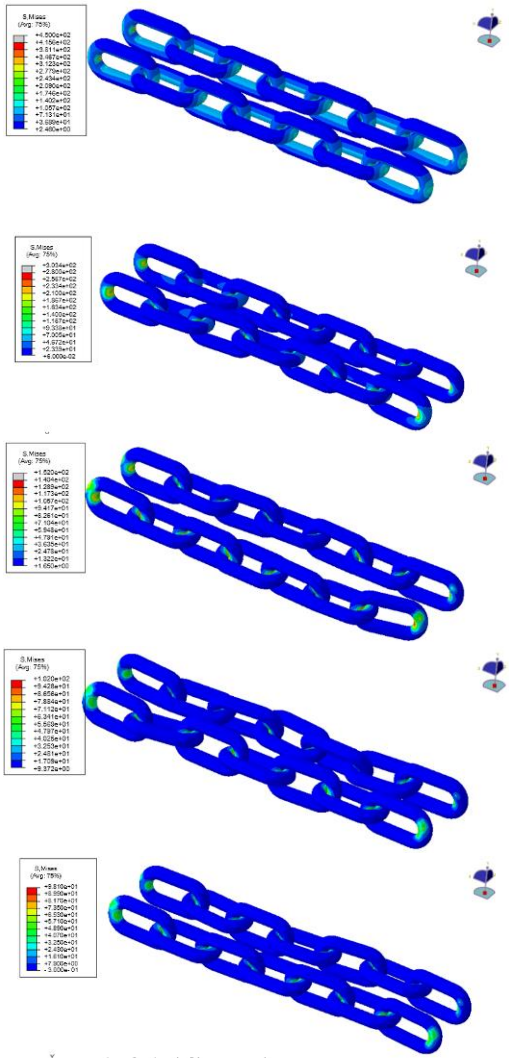

Figure 19 Mises stress distribution of chain between two scrapers

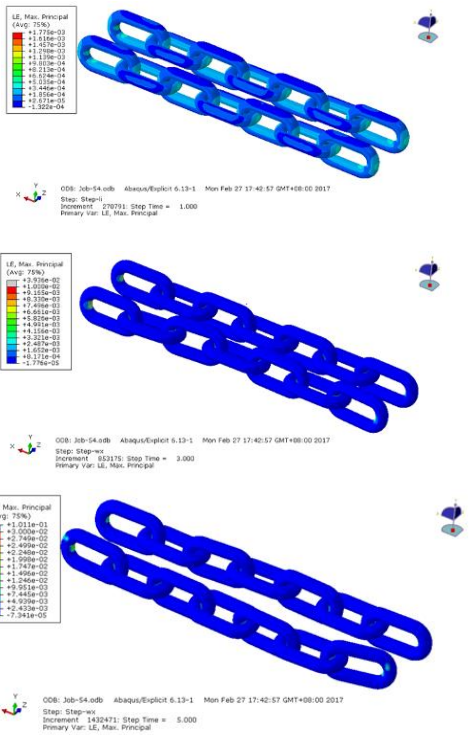

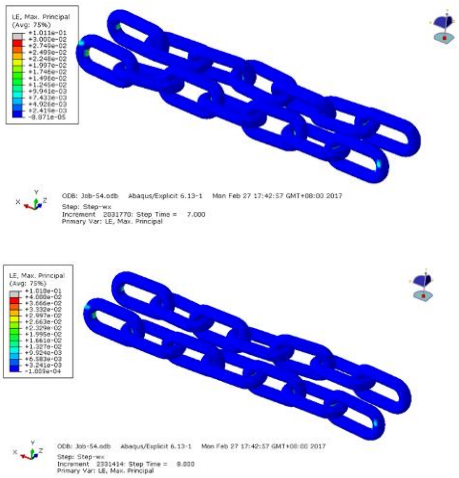

Figure 20 Maximum strain distribution of chain between two scrapers

At the moment of 1.0s chain, the stress and strain of the two chains suddenly increase. The maximum stress and strain appeared in 2.0 s, and then each link twisted violently under the influence of scraper torsional pendulum vibration with the change of time. The inner side of the chain produces strain under the action of compressive stress, and the outside of the chain produces strain under the action of tensile stress. The stress and strain at the contact part between the link and the link is the largest, and the maximum stress is 4.51e+2MPa, which becomes 1.1e-1. In the process of the clip chain, the chain behind the card chain is forced to pull, collide with each other and transmit vibration, resulting in stress concentration at the contact of the chain link. The stress and the resulting strain in the arc segment of the chain are more obvious. Different monitoring points are selected on the two chains in order to more directly observe the changes of stress and strain with time. The changes of stress and strain of each monitoring point in chain 1 and 2 with time are shown in figs. 21 and 22, respectively.

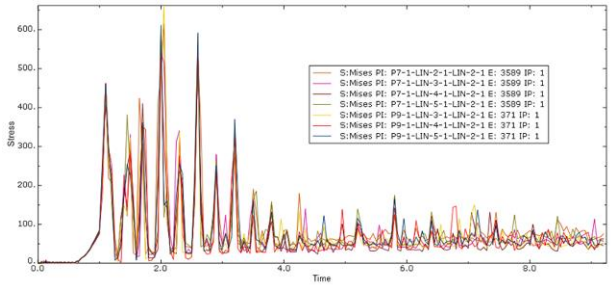


(a) Stress change

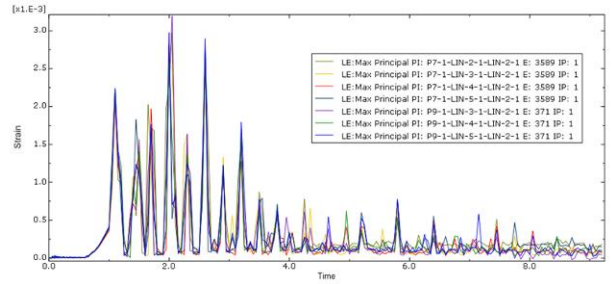


(b) Strain change

Figure 21 The change of stress and strain in each of the monitoring points in chain 1 under the working condition 2

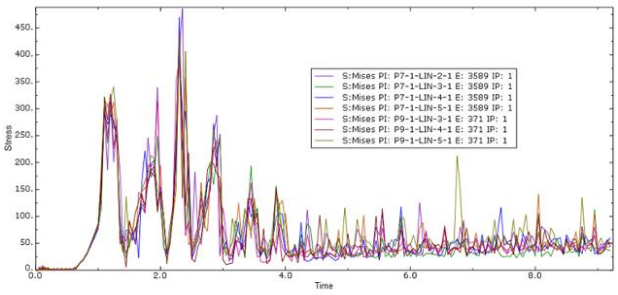


(a) Stress change

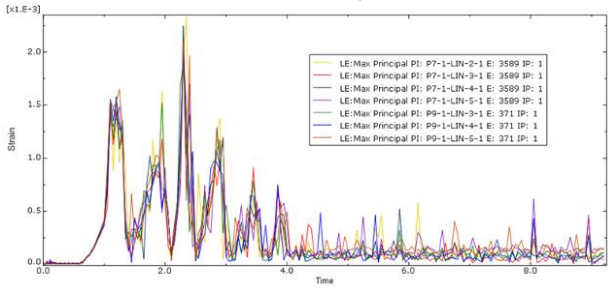


(b) Strain change

Figure 22 The change of stress and strain in each of the monitoring points in chain 2 under the working condition 2

Through the analysis of the time variation curves of the stress and strain of each monitoring point in chain 1 and chain 2, it is known that the stress and strain of the monitoring point of the chain gradually increased from zero to the rated value during the period of 0.0 to 1.0s, because this process is the pretightening process of the chain. The stress and strain of each link in the chain fluctuated violently when the load of the chain was increased during 1.0-3.0s, and reached the maximum value at 2.0s. When the load of the clip chain is removed after 3.0s, the fluctuation of the stress and strain of each link in the chain gradually weakens. The fluctuation of stress and strain shows that under the action of abnormal bias load, the chain links have not only one collision, but a state of near equilibrium due to the repeated process of collision and departure. The maximum stress is concentrated in the first eight wave peaks, showing the characteristics of instantaneous impact, so the chain process is accompanied by huge instantaneous shock and periodic collision, which is equivalent to a damped vibration process. The initial impact does great damage to the chain link, and the subsequent repeated vibration is equivalent to fatigue, which will aggravate the damage of the chain link. Under the condition of chain clamping, the maximum stress in the first chain monitoring point is 582.5MPa, the second chain monitoring point is 616.3MPa, the maximum strain value in the first chain monitoring point is 2.85e-3, and the maximum strain value in the second chain monitoring point is 3.12e-3. Under the condition of clamping chain, it can cause the severe torsional pendulum vibration of the scraper chain system, and make the stress and strain of each link in the chain fluctuate strongly. If the machine is not stopped in time or the load of the chain is eliminated, it is easy to cause one of the chains to be broken, and then both chains are broken.

# 5 Experimental study.

## 5.1 Experimental equipment for mechanical characteristics of scraper conveyor

Experimental research is carried out on the simulation test-bed of fully mechanized mining equipment built by the R & D (experimental) center of China's National Energy Administration(as shown in figure 23). The test-bed simulates the environment of underground coal mining face at 1:1, and is mainly composed of mining equipment and experimental testing equipment, such as simulated coal wall, shearer, scraper conveyor, hydraulic support, etc. The parameters of SGZ1000/ 1050 scraper conveyor used in the test bench are shown in Table 1.

Figure 23 Complete sets of equipment for fully mechanized coal mining

Table 1 Main parameters of SGZ1000/1050 scraper conveyor

| Technical parameters | Parameter value | Technical parameters | Parameter value |
|---|---|---|---|
| Design length | 250m | Scraper chain speed | 1.25m/s |
| Actual length | 70m | Middle slot specification | 1500*1000*360mm |
| Capacity | 2000t/h | Chain center distance | 200mm |
| Motor | YBSD-525/263-4/8 | Chain specification | 38*137 |
| Power | 525kW | Chain type | Medium double strand |

## 5.2 Testing device

The stress-strain testing device of the chain link is set up in the test-bed. The chain stress test mainly includes the fluctuation of dynamic tension of chain under different working conditions and the change of tension value. When monitoring, stick the strain gauge on the chain, as shown in figure 24, the strain gauge is installed. In order to make the scraper and the chain link engage more accurately, the strain gauge is attached to the outside of the flat chain ring, and the protection treatment is required at the same time.

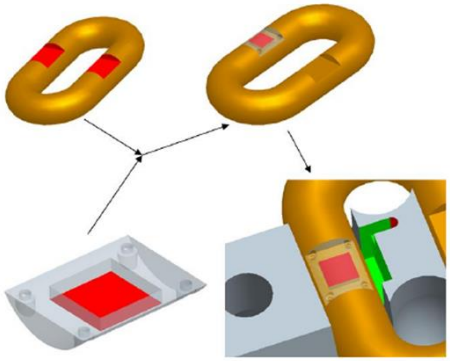

(a) Installation diagram

(b) Installation drawing

Figure 24 Installation diagram of strain gauge

The wireless data acquisition module is placed inside the scraper and connected with the strain gauge. The wireless data acquisition module collects the change value of the strain gauge in real time and transmits it to the gateway through the wireless transmitting antenna. The interior of the original scraper is modified to produce a space where wireless acquisition modules, strain gauges and connecting wires can be installed [20]. The schematic diagram of scraper modification and wireless data acquisition module installation is shown in figure 25.

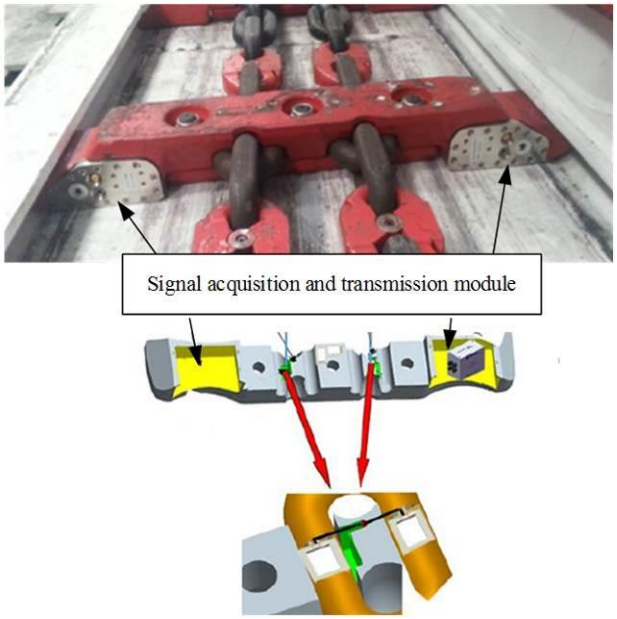


Figure 25 Sketch map of data collection and transmission system

## 5.3 Sensor calibration

Before testing, it is necessary to calibrate the data of each sensor in order to obtain the stress of the chain link through the tested strain value. The calibration process is to apply loads of different amplitudes to the sensor, and the load calculation

formula is obtained by fitting the strain values obtained. Take the chain link tension sensor numbered C14035001-1 as an example for data calibration. The rated load of 400kN, 600kN and 800kN is applied to the chain link using loading equipment, and the measured micro-strain data is shown in Table 2.

Table 2 C14035001-1 sensor calibration data

| Loading value (KN) | Micro strain (με) |
|---|---|
| 400 | 2427 |
| 600 | 3471 |
| 800 | 5066 |

By fitting the loading value and micro-strain data, the calibration of the sensor is completed, and the relationship between the link force and the micro-strain measured by the sensor is obtained:

$$F_{C14035001-1} = \text{-}1.781e-5\times CH^{2}_{C14035001-1} +0.3167\times CH_{C14035001-1} - 598.8 \quad (11)$$

Among them, CHC14035001-1 is the micro-strain measured by C14035001-1 sensor, and FC14035001-1 is the strain corresponding load value, KN.

## 5.4 Analysis of experimental results

The calibrated link tension sensor is used to test the link tension under light load and medium load respectively. During several light load tests, the micro-strain of the chain link tension sensor and the converted tension curve are shown in figure 26.

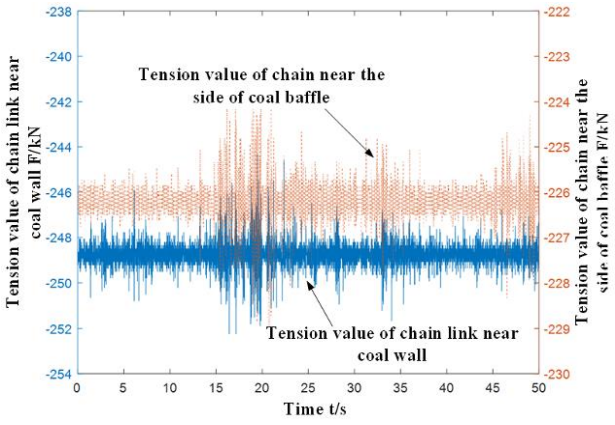


(a) First test

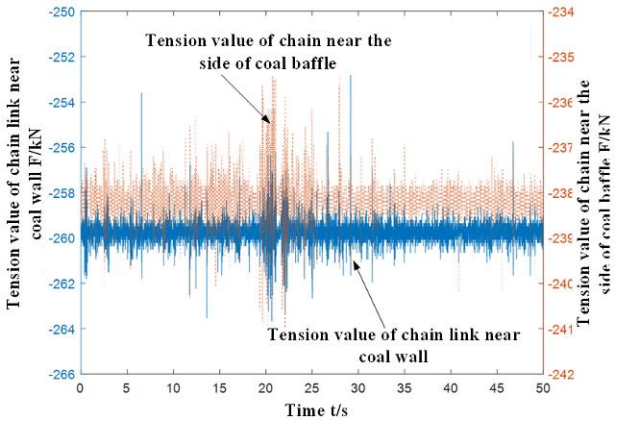


(b) The second test

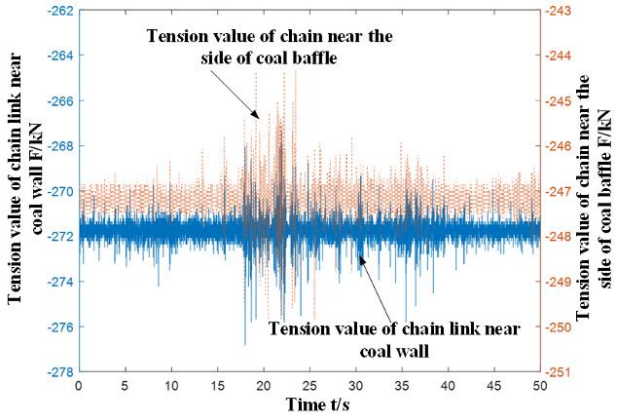


(c) The third test

Figure 26 Data acquisition of chain tension sensor under light load condition

The multi-test data under light load conditions are collected when the scraper installed with the sensor runs to different positions. The first test data acquisition point is closest to the tail, and the eighth test data acquisition point is closest to the nose. The tension value of the link measured by the sensor increases gradually in the multiple test data. The average tension values of chain links near the coal wall are 249.4kN, 260.5kN, 272.4kN, 277.8kN, 287.1kN, 305.6kN, 318.2kN and 323.6kN, respectively. The average tension values of side chain links near the coal baffle are 226.2kN, 238.7kN, 247.1kN, 260.3kN, 267.2kN, 283.7kN, 290.2kN and 309.8kN, respectively. Compare the experimental test data with the theoretical calculation data, as shown in figure 27.

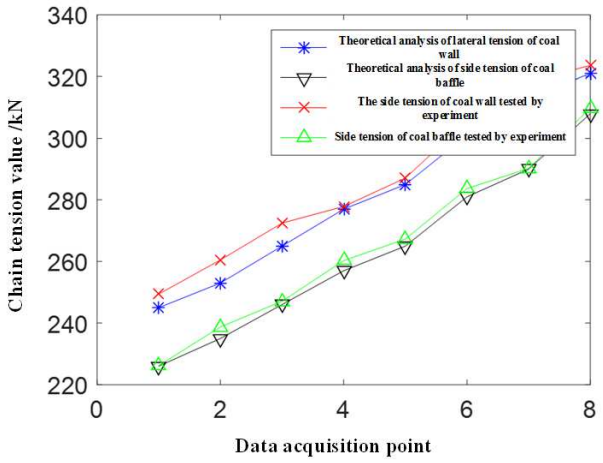


(a) Theoretical analysis of chain tension and comparison of test data

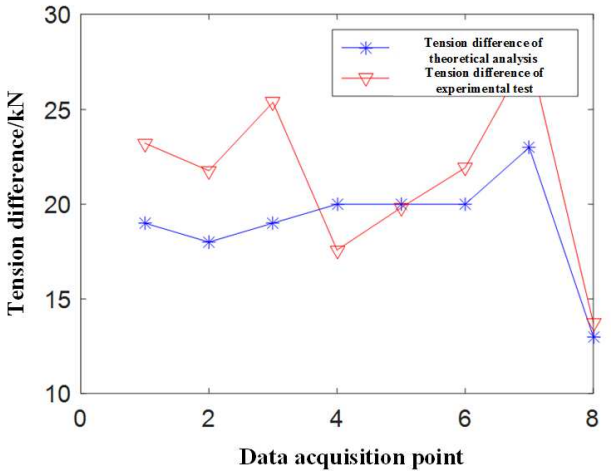


(b) Theoretical analysis of chain tension difference and comparison of test data

Figure 27 Comparison between the experimental test data and the theoretical analysis data under light load condition

In each data acquisition, the average difference of tension between the side chain link near the coal wall and the side chain near the coal baffle is 21.4kN, and the extreme value is 27.9kN. According to the theoretical analysis, the average difference of tension between the side chain link near the coal wall and the side chain near the coal baffle is 19.2kN, and the extreme value is 23.2kN. There are errors of 11.3% and 16.8% between the experimental results and the theoretical analysis results. When testing many medium load conditions, the micro-strain and the converted tension curve of the chain link tension sensor are collected as shown in figure 28.

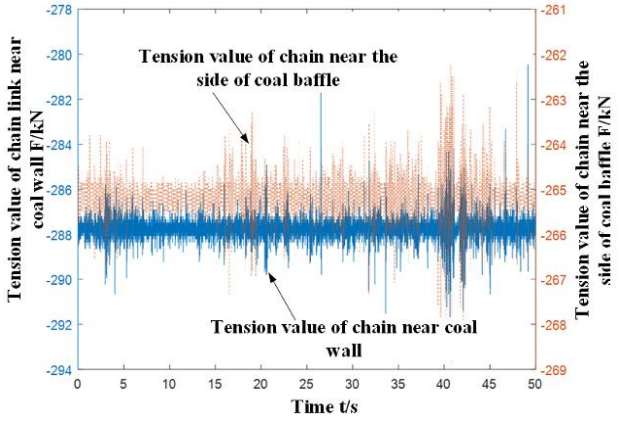


(a) First test

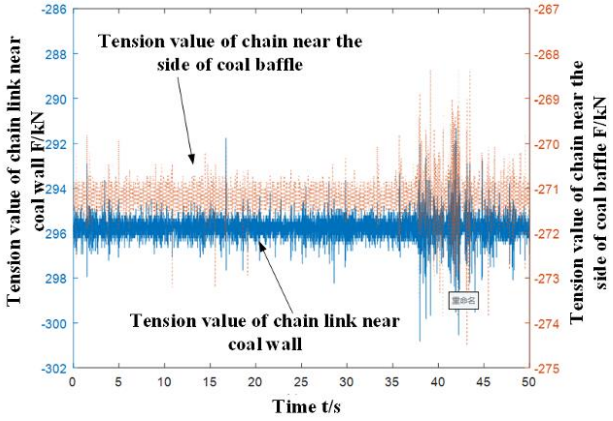


(b) The second test

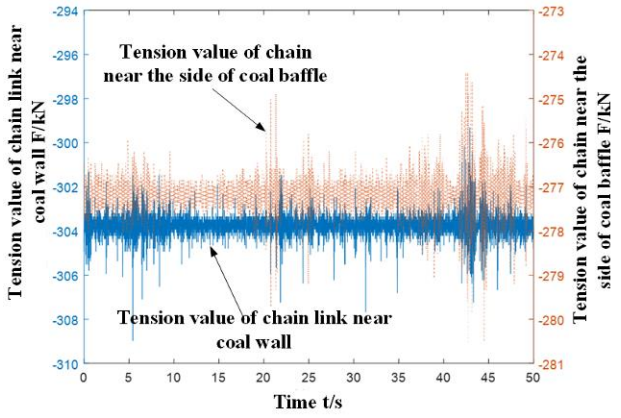


(c) The third test

Figure 28 Data acquisition of chain tension sensor under middle load condition

Under the medium load condition, the tension value of the link measured by the sensor increases gradually in the multiple test data. The average tension values of chain links near the coal wall are 288.3kN, 296.4kN, 304.6kN, 318.2kN, 330.6kN, 334.5kN, 352.1kN and 358.2kN, respectively. The average tension values of side chain links near the coal shield are 265.2kN, 271.6kN, 277.1kN,

290.5kN, 307.7kN, 305.4kN, 320.5kN and 333.1kN, respectively. Because the coal material driven by the scraper under the medium load condition is more than that under the light load condition, the tension value of the chain link detected by the tension sensor on both sides of the scraper is higher than that under the light load condition. Compare the experimental test data with the theoretical analysis data, as shown in figure 29.

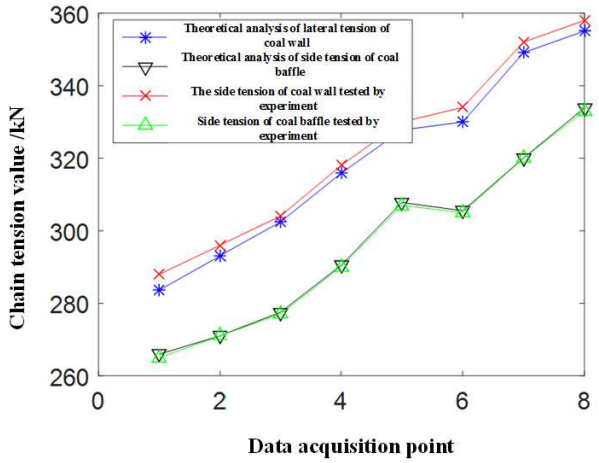


(a) Theoretical analysis of chain tension and comparison of test data

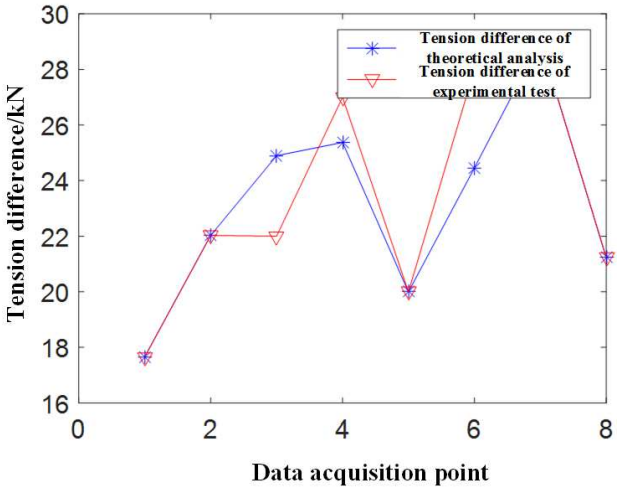


(b) Theoretical analysis of chain tension difference and comparison of test data

Figure 29 Comparison between the experimental test data and the theoretical analysis data under middle load condition

In each data acquisition, the average difference of tension between the side chain link near the coal wall and the side chain near the coal baffle is 26.5kN, and the extreme value is 32.3kN. According to the theoretical analysis, the average difference of tension between the side chain link near the coal wall and the side chain near the coal baffle is 23.1kN, and the extreme value is 29.4kN. There are errors of 13.8.3% and 10.3% between the experimental results and the theoretical analysis results.

# 6 Conclusion

In this paper, taking the Φ 38 × 137 chain of SGZ1000/ 1050 scraper conveyor as the research object, the finite element models of two ring chains are established by using the nonlinear dynamics finite element software ABAQUS, and the instantaneous contact process of the ring chain at both ends under the constraint of torsional pendulum vibration boundary conditions is dynamically simulated.

(1) under the material loading condition, the maximum values of stress and strain in the two chain monitoring points are 258.5MPa, 1.25e-3 and 270.6MPa, 1.32e-3, respectively. Although there is little difference between the stress and strain of the two links in the corresponding position of the two chains under the material loading condition, the cargo load excitation is the type of load excitation with the highest frequency. Long-term unbalanced material partial load will cause the stress and strain difference of the two links in the corresponding position in the chain to become larger and larger. In the end, one of the chains was broken, followed by both chains.

(2) Under the condition of chain clamping, the maximum values of stress and strain in the monitoring points of the two chains are 582.5MPa, 2.85e-3 and 616.3MPa, 3.12e-3, respectively. Under the condition of clamping chain, it can cause the severe torsional pendulum vibration of the scraper chain system, and make the stress and strain of each link in the chain fluctuate strongly. If the machine is not stopped in time or the load of the chain is eliminated, it is easy to cause one of the chains to be broken, and then both chains are broken.

The research results of this paper can provide a basis for chain life prediction and safety factor calculation.

# Acknowledgments

The authors would like to express their thanks

for the financial support provided by the National Natural Science Foundation of China (No. 51774162), Liaoning Provincial Department of Education Project (LJ2020QNL012).

## Contributors

Chun-xue XIE and Jun MAO designed the research. Miao XIE processed the corresponding data. Chun-xue XIE wrote the first draft of the manuscript. Zhi-xiang LIU helped to organize the manuscript.

## Conflict of interest

Chun-xue XIE , Zhi-xiang LIU, Miao XIE, Jun MAO declare that they have no conflict of interest.

## Reference

[1] Sikora W.The inhomogeneity of drive device of efficient scraper conveyor[J]. Przegl .Gorn. 1993(4):23-26.

[2] Murphy C J, Bliss R E.Method and apparatus for belt conveyor load tracking: U.S. Patent 5,335,777[P]. 1994-8-9.

[3] Katterfeld A., Gröger T., Minkin A..Discrete element simulation of transfer stations and their verification[C]. 9th International Conference on Bulk Materials Storage, Handling and Transportation, 2007, Newcastle, NSW, Australia.

[4] Dolipski M, Remiorz E, Sobota P. Dynamics of Non-Uniformity Loads of Afc Drives[J]. Archives of Mining Sciences, 2014, 59(1): 155-168.

[5] Li Weikang, Mao Jun, Li Jiangang, et al. Optimization of scraper spacing in scraper conveyor [J]. Journal of Liaoning Technical University, 2008, 27 (6):912-914.

[6] Xu Guangming, Yang Weihong. Calculation and analysis of running resistance of scraper conveyor [J]. coal mine machinery, 2009, 30 (1):3-5.

[7] Han Dejiong, Li Donghao, Song Weigang. Differential numerical method and computer simulation of dynamic problem of scraper conveyor [J]. mining machinery, 2009, 37 (11):22-26.

[8] Liu Wensheng, Huang Wenbin. Analysis of running resistance of scraper conveyor [J]. Heilongjiang science and technology information, 2010, (15):36-36.

[9] Ma Shuhuan. Dynamic analysis of belt conveyor scraper in loading amount of [J]. coal mine machinery, 2011, 32 (1):192-193.

[10] Cai Cai Liu. Transportation and mechanical behavior of coal bulk material in the middle trough of scraper conveyor [D]. Taiyuan: Taiyuan University of Technology, 2016.

[11] Liu Wei. Calculation and analysis of tension and safety factor of conveyor chain [J]. mechanical engineer, 2016, (10):158-159.

[12] Wang Yabin. Study on the control system of controllable starting device of heavy scraper conveyor [D]. Taiyuan: Taiyuan University of Technology, 2016.

[13] Dolipski M, Remiorz E, Sobota P. Determination of Dynamic Loads of Sprocket Drum Teeth and Seats by Means of a Mathematical Model of the Longwall Conveyor[J]. ARCHIVES OF MINING SCIENCES ,2012,57(4): 1101-1119

[14] Mao Jun. Dynamic behavior analysis and control theory of scraper conveyor [D]. Fuxin: Liaoning Technical University, 2006.

[15] Zhi, Jie-ying, Wang, Shen-ping, Wang, Hai-qing ,et al. Analysis on Energy Loss of Rubber under Dynamic Load[J].ACTA POLYMERICA SINICA,2017, (4): 708-715.

## Data availability statement

• All data generated or analysed during this study are included in this published article [and its supplementary information files].

## Supplementary Files

This is a list of supplementary files associated with this preprint. Click to download.

- testdata.zip